Original Article

JCBFM

What does computational fluid dynamics tell us about intracranial aneurysms? A meta-analysis and critical review

Khalid M Saqr[1,2], Sherif Rashad[3,4], Simon Tupin[1],
Kuniyasu Niizuma[3,4,5], Tamer Hassan[6], Teiji Tominaga[4] and
Makoto Ohta[1]

Abstract

Despite the plethora of published studies on intracranial aneurysms (IAs) hemodynamic using computational fluid dynamics (CFD), limited progress has been made towards understanding the complex physics and biology underlying IA pathophysiology. Guided by 1733 published papers, we review and discuss the contemporary IA hemodynamics paradigm established through two decades of IA CFD simulations. We have traced the historical origins of simplified CFD models which impede the progress of comprehending IA pathology. We also delve into the debate concerning the Newtonian fluid assumption used to represent blood flow computationally. We evidently demonstrate that the Newtonian assumption, used in almost 90% of studies, might be insufficient to describe IA hemodynamics. In addition, some fundamental properties of the Navier–Stokes equation are revisited in supplementary material to highlight some widely spread misconceptions regarding wall shear stress (WSS) and its derivatives. Conclusively, our study draws a roadmap for next-generation IA CFD models to help researchers investigate the pathophysiology of IAs.

Introduction

With 50–60% mortality after rupture and 30–40% dependence rate amongst survivors,[1] intracranial aneurysms (IAs) are one of the most feared cerebrovascular pathologies. While treatment options are very well established in the medical field, either in the form of surgical clipping, with its modifications based on the location, geometry, complexity, etc., or endovascular treatment with its various forms,[2,3] there exists a dilemma that is yet to be solved. Approximately 50–80% of IAs do not rupture in the individual's lifetime.[4] While it is the standard to treat all ruptured aneurysm cases upon detection,[3] unruptured aneurysms make up for a difficult decision making. Unruptured aneurysms can be followed for certain period of time, especially smaller sized ones.[5] However, while changes in aneurysm morphology or size are warning signs against impending rupture, there is no telling how fast such changes will occur[6–8] and treating unruptured aneurysms is certainly not a risk-free option.[9–11]

[1]Biomedical Flow Dynamics Laboratory, Institute of Fluid Science, Tohoku University, Sendai, Miyagi, Japan
[2]Department of Mechanical Engineering, College of Engineering and Technology, Arab Academy for Science, Technology and Maritime Transport, Alexandria, Egypt
[3]Department of Neurosurgical Engineering and Translational Neuroscience, Tohoku University Graduate School of Medicine, Sendai, Miyagi, Japan
[4]Department of Neurosurgery, Tohoku University Graduate School of Medicine, Sendai, Miyagi, Japan
[5]Department of Neurosurgical Engineering and Translational Neuroscience, Graduate School of Biomedical Engineering, Tohoku University, Sendai, Japan
[6]Department of Neurosurgery, Alexandria University School of Medicine, Azarita Medical Campus, Alexandria, Egypt

Corresponding authors:

Sherif Rashad, Department of Neurosurgery, Tohoku University Graduate School of Medicine, 1-1 Seiryo-machi, Aoba-ku, Sendai 980-8574, Japan.
Email: sherif_rashad@hotmail.com; sherif@nsg.med.tohoku.ac.jp
Khalid M Saqr, Biomedical Flow Dynamics Laboratory, Institute of Fluid Science, Tohoku University, Sendai 980-8577, Japan.
Email: k.saqr@tohoku.ac.jp

Therefore, taking chances in IA care do not only risk the livelihood of patients, but it also multiplies the cost of healthcare delivery as well as burden of the healthcare services.[12] Given the aforementioned factors, the cerebrovascular research into IA pathobiology needs not only to answer questions regarding the formation and growth of IAs, but also seeks to answer why and how aneurysms rupture. A question that may seem direct at the first glance, yet it is made complex by the intertwining relationships between biological and physical factors that are yet to be fully understood.

Therefore, to understand the pathobiology of IAs, it is imperative to understand the different flow regimes in the intracranial vessels and inside the IAs and how they affect the ECs and consequently the vessel wall. To understand the blood flow dynamics, researchers had to turn to the field of fluid mechanics, modifying their tools to be used for the study of blood flow in various vessels, connecting the dots and ultimately searching for a holistic understanding of the pathology of IAs. The most famous and ubiquitous of these tools used nowadays is computational fluid dynamics (CFD) analysis.

It is a very well established fact that endothelial cells (ECs) sense the blood flow via a variety of cell surface and intracellular mechano-sensors,[13] and they transmit signals of the blood flow into cellular response that derives the vascular homeostasis.[13,14] Any abnormality in the blood flow induces pathologic responses in the ECs, causing vascular diseases such as atherosclerosis.[15–17] ECs also were shown to transmit flow signals to the underlying cells in the vascular wall, such as vascular smooth muscle cells, via exosomes and microRNA transfer.[17] Moreover, ECs were shown to respond to wall shear stress (WSS) via several mechanobiological mechanisms.[18,19] From such observation, it is safe to base the model of IAs formation, growth and rupture on an interaction between blood flow and ECs. Even in ruptured aneurysms where the ECs are lacking,[20] such a finding must be linked with ECs death and shedding, possibly leading to an accelerated aneurysmal wall weakening and eventual rupture from the loss of the normal buffer between the flow and the wall (i.e. the ECs and their intercellular junctions[15,21,22]). ECs damage is associated with internal elastic lamina pathophysiologic changes and damage, as well as inflammatory cell recruitment, via cytokines and other molecules, and aneurysm wall degeneration or sclerosis.[23,24] Moreover, abnormal collagen fibers in the aneurysm wall indicate a failed wall remodeling.[25] Indeed, differences in wall inflammation and internal elastic lamina were observed between ruptured and unruptured aneurysms.[24] This indicates that the pathophysiology of IA, while might start at the level of ECs, is in fact spanning all the layers of the wall and should be studied with this in mind.

Early works on IA hemodynamics

There is almost a consensus in literature on the prime role of wall shear stress (WSS) as the most profound hemodynamic parameter affecting aneurysm fate. Such consensus was established following to the early work of Ferguson et al.[26–28] in the early 1970s, in which they constructed *in vitro* flow models of IA geometries guided by craniotomy observations. Their work was revolutionary at the time as they suggested that transition to turbulence occurs in IA and lead to degeneration of internal elastic lamina and rapid weakening of the aneurysm wall.[27] Their work was followed by a series of studies by Steiger et al.,[29] Liepsch et al.,[30] Gonzalez et al.[31] and Kim et al.[32] which settled the consensual WSS theory in IA hemodynamics.[33] Steiger's group work was the first recorded *in vitro* measurements of IA flow fields using laser techniques.[34,35] Until that time in the late 1970s to early-mid 1980s, *in vitro* works postulated that blood flow in IA exhibits turbulence and transitional features which contribute to the IA growth and wall deterioration,[26,36,37] which is in line with recent biological findings.[15] Moreover, such early works considered the non-Newtonian effects of IA hemodynamics influential.[34,38–40] Wall shear stress in these studies was only a measure of the flow at the IA wall, not an independent variable that thought to control IA pathophysiology and mechanotransduction.

CFD and current controversies

In the past two decades, CFD has been an effective research tool for investigating numerous aspects of IA,[10,41–43] most importantly growth and rupture mechanisms and their relation with vascular hemodynamics.[44–46] IA CFD simulations mostly aim to evaluate the morphologic factors and hemodynamic forces on the aneurysm walls[47] which trigger a set of vascular remodeling mechanisms[48,49] leading to IA progression and possible rupture.[50] Moreover, CFD is used to study the growth and rupture of IAs, as well as assessing different endovascular treatment modalities[51] and validating new endovascular devices.[8,10,11] While CFD and flow studies have significantly improved our understanding of vascular pathologies such as atherosclerosis and that the flow perturbations at bifurcations were linked to evident pathobiological processes,[15,52] such an understanding is yet to be reached in the field of IAs research, and a large gap of knowledge still exist. This gap of knowledge is in part due to the complexity of blood flow in IAs as well as controversies regarding the actual flow regime causing rupture.[10,53] These controversies are related to the actual inducer of aneurysm rupture, whether it is high or low WSS[54] and to the actual viscosity model that should be adopted to model the blood flow, whether Newtonian or non-Newtonian.[55]

Moreover, there are controversial issues pertaining to the validity of the some of the parameters used in the analysis of the flow regimes, such as the vector calculations of WSS, that need to be addressed.[56] Thus, we believe it is vital to evaluate the tools we are using to understand IAs, highlighting the controversies and unveiling the shortcomings in our approaches and tools to be able to progress and improve.

The optimality principle, proposed by Murray,[57] which is often used in CFD simulations, correlates arterial hemodynamics to the dimensions of individual arteries via a power-law correlation. The major consequence of such principle is that any vascular remodeling due to hemodynamic changes should eventually be attributed to deviation from the optimal geometrical parameters. However, Murray's principle was derived assuming steady laminar flow in straight vessels, and no direct communication between arteries of the same rank. This is not the case in the circle of Willis or any intracranial vessel.[58] *In vivo* evidence showed that Murray's law could be valid on the scale of the system; however, it is incapable of accurately predicting *in vivo* WSS measurements in intracranial arteries.[59–61] This leaves the coupled interaction between IA and hemodynamics, on different scales, an open question beyond any geometrical characterization attempts. Consequently, this coupled interaction inherits multi-layered complexity from the morphological sophistication of the circle of Willis,[62] let alone the fluid dynamics intricacies driven by the multi-harmonic blood flow waveform which exhibits phase shifts,[63,64] non-linear dynamics,[65] and a multitude of biochemical, biophysical and mechanobiological processes.[66]

Aim and motivation

The aim of this work was to evaluate the current standpoint of the CFD research on IAs by performing a meta-analysis of all the literature concerning IA hemodynamics and critically reviewing it. The ultimate aim is to evaluate the tools and techniques used in order to provide a recipe for improvement. Such an improvement will enhance the outcome of CFD research and provide a better link between the physics of the blood flow and the biological processes observed in the IAs. Through our meta-analysis, we came across several open-ended questions that we will try to either answer or highlight and present to the readers. These questions include:

1. What are the current trends in IA hemodynamics research?
2. Does the Newtonian assumption, widely used in CFD models, accurately represent physiological conditions?
3. What is the actual *flow regime* of blood in intracranial aneurysm?
4. In the light of current controversies in CFD literature, what is the clinical and biological relevance of such models with respect to the initiation, growth and rupture of intracranial aneurysm?

We aim to tackle these questions based on the contemporary paradigm driven from published studies in the field. The final target of this meta-analysis and critical review is to stimulate debate, critical analysis and falsification of such paradigm to advance IA CFD models towards future theoretical and applied relevance.

Methods and data

Meta-analysis on IA CFD studies

We obtained the literature records and references from Scopus bibliographic database using TITLE-ABS-KEY search function with the following search terms:

– "Cerebral aneurysm" OR "Intracranial aneurysm"
– AND "Hemodynamics" OR "Flow dynamics" OR "Blood flow"

Then we classified the references corpus, which contained 1733 published articles, manually through reading the abstracts and conclusions and grouping the articles into groups based on the technique of study (CFD or other techniques including *in vivo, in vitro* studies and animal models). Then, the CFD references, which counted 795 papers were analyzed in detail for technique, methods and models used. All the references obtained from the meta-analysis search records were classified according to their relevance to the topic of this study. The details and findings of such classification and analysis are presented in the Results and Discussion section. The meta-analysis was conduced in line with the PRISMA guidelines.[67]

Meta-analysis criteria and mathematical model for WSS comparison

Literature records have been searched on Scopus® database for studies reporting the dimensions and flow rates or velocities of intracranial and cerebral arteries in healthy subjects. Patients suffering from intracranial aneurysm are not necessarily suffering from other disorders that could alter their blood viscosity. In addition, blood flow velocity inside aneurysms is often much less than such of the parent artery. Hence, it is valid to assume that the blood viscosity behavior in aneurysm patients is similar to such in healthy patients

Table 1. Hypothesis testing of the Newtonian assumption based on WSS calculations from *in vivo* radiological measurements.

Model	Mean (Pa) ± Variance (Pa)	P-value ($P_c = 0.05$)
Newtonian	3.073 ± 5.125	∞
Power-law	2.843 ± 2.690	0.046
Carreau	4.688 ± 10.985	4×10^{-10}
Carreau-Yasuda	3.214 ± 3.752	0.021
Casson	3.329 ± 4.867	1×10^{-20}
Cross	3.965 ± 7.573	1×10^{-12}

Note: The sample population consists of the WSS values from all the arteries in the meta-analysis.

for the scope of the present study. The studies were selected such that each study provide synchronized readings for the blood velocity (m/s) or flow rate (m^3/s) with the vessel diameter (m) or cross-sectional area (m^2) during specific instants of the cardiac cycles or as mean values for one cardiac cycle. The details of such studies are summarized in Supplementary Table 1. A summary of the measurements is plotted in Supplementary Figure 1. The collected measurements from selected studies were used to compute the shear rate (s^{-1}) based on the exact Hagen-Poiseuille solution of Newtonian incompressible flow[68–70] as following

$$Q = \pi R^2 \frac{v_{max}}{2} \tag{1}$$

$$\dot{\gamma} = \frac{\tau_w}{\mu} = \frac{2 v_{max}}{R} \tag{2}$$

For shear thinning fluids, where velocity profiles deviate from the parabolic profile shown by the Hagen-Poiseuille solution, shear rate values should be corrected using the Weissenberg–Rabinowitsch (W-R) shear-thinning correction[71,72]

$$\dot{\gamma}_{NN} = \frac{\dot{\gamma}}{4}\left[3 + \frac{1}{n}\right] \tag{3}$$

where *n* is the shear-thinning index of the fluid, as presented by the rheological model that is used to compute the non-Newtonian viscosity. Hence, wall shear stress (WSS) was calculated for the Newtonian viscosity assumption as

$$\tau_w = \mu \dot{\gamma} \tag{4}$$

and for different non-Newtonian models as

$$\tau_w = \mu_{eff} \dot{\gamma}_{NN} \tag{5}$$

where μ_{eff} is the effective viscosity as calculated from each of the non-Newtonian models

Power-law (PL)[73]:

$$\mu_{eff} = K\dot{\gamma}^{n-1} \tag{6}$$

where $K = 0.01467$ and $n = 0.7755$.

Carreau (C)[74–76]:

$$\mu = \mu_\infty + (\mu_0 - \mu_\infty)\left[1 + (\lambda\dot{\gamma})^2\right]^{\frac{n-1}{2}} \tag{7}$$

where $\mu_\infty = 0.00345\,\text{Pa.s}$, $\mu_0 = 0.056\,\text{Pa.s}$, $\lambda = 3.313\,\text{s}$ and $n = 0.3568$.

Carreau-Yasuda (C-Y)[77]:

$$\mu = \mu_\infty + (\mu_0 - \mu_\infty)[1 + (\lambda\dot{\gamma})^a]^{\frac{n-1}{a}} \tag{8}$$

where $\mu_\infty = 0.0022\,\text{Pa.s}$, $\mu_0 = 0.022\,\text{Pa.s}$, $\lambda = 0.11\,\text{s}$, $a = 0.644$ and $n = 0.392$.

Casson (CS)[78,79]:

$$\mu = \left(\frac{1}{\dot{\gamma}}\right)\left[K_0(c) + K_1(c)\sqrt{\dot{\gamma}}\right]^2 \tag{9}$$

where $K_0(c) = 0.1937\,Pa^{\frac{1}{2}}$, $K_1(c) = 0.055\,Pa^{\frac{1}{2}}$. The Casson yield stress $K_0(c)$ is considered here proximal to the shear-thinning index of blood.[80]

Cross (CR)[81]:

$$\mu = \mu_\infty + \frac{(\mu_0 - \mu_\infty)}{(1 + (\lambda\dot{\gamma})^n)} \tag{10}$$

where $\mu_\infty = 0.0036\,\text{Pa.s}$, $\mu_0 = 0.126\,\text{Pa.s}$, $\lambda = 8.2\,\text{s}$ and $n = 0.64$.

Hypothesis testing and statistical analysis

The null hypothesis of the WSS comparative study was that the Newtonian and non-Newtonian calculations of WSS are similar with no significant differences. This is the essence of using Newtonian viscosity in CFD simulations. Paired *t*-tests were conducted to compare the Newtonian (N) model with each of the five non-Newtonian rheological models that are commonly used in literature, given by equations (6) to (10).

In vivo calculations of WSS in IAs

The validation of CFD models against *in vivo* measurements is a crucial task, yet not commonly practiced in the IA hemodynamics research community. Here, we explored the studies which reported *in vivo* estimations of WSS in IA. In principle, different radiological
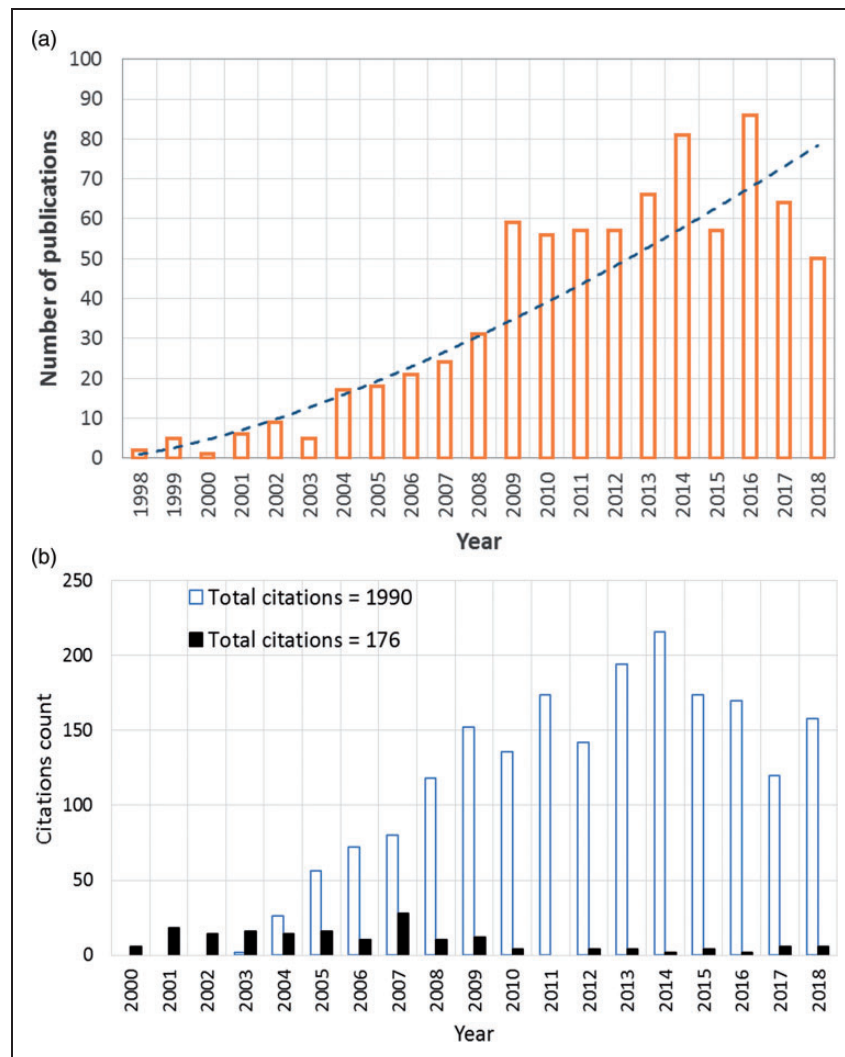
Figure 1. The rise of simplified CFD models of IA hemodynamics during the past two decades. (a) Exponential growth in the use of CFD as a research tool in aneurysm hemodynamics based on Scopus® database. Search query available in the supplementary materials. (b) Comparison of the citation counts (2000–2018) from Scopus® bibliographic database between the early *in vitro* works reporting complex IA flow physics (black column indicates total annual citations for references[34,38,39]) and subsequent CFD models adopting simplified assumed flow physics (blue outlined column indicates total annual citations of references[85,87,234]).

techniques such as MRI or transcranial color Doppler (TCCD) are used to measure the velocity time-series in the region of interest. Then, post-measurement calculations are conducted to estimate WSS as function of the measured velocity series and geometry. A comparative analysis based on six studies, as summarized in Table 2, which reported *in vivo* post-measurement calculations of WSS in IAs was conducted. The criteria for selecting the six studies were as following:

– Usage of high-fidelity multidimensional radiological technique (3D/4D MR)
– Study must report quantitative and qualitative results
– The method of computing WSS sufficiently explained in each study in terms of adequate use of

measurements data and fully explained mathematical model.

The values of WSS presented in such studies are reviewed and analyzed. The purpose of this analysis is to explore the hemodynamics of IA as detected *in vivo* to provide benchmark to discuss the current hypothesis proposed by CFD studies.

Results and discussion

CFD and deviation towards simplification

In the 1990s, and with the large leap in CPU speed and radical increase in PC availability, CFD has emerged as

Table 2. Summary of in vivo estimations of hemodynamic parameters in IA.

Reference	WSS_{rel} (%)	WSS_{IA} (Pa)	U_{sys} (m/s)	$\dot{\gamma}$ (1/s)
Meckel et al.[234]	24.6–116.6	–	0.06–0.59	–
Isoda et al.[235]	46.9–76.4	1.16–2.22	0.0–0.5	0.0–1600
Schnell et al.[236]	–	0.5–2.25	0.4–1.01	–
Blankena et al.[237]	–	0.1–8.1	–	–
Zhang et al.[238]	–	0.63–1.09	–	–
Boussel et al.[239]	–	0.01–0.2	0.0–0.1	–

Note: WSS_{rel} is the ratio between average WSS in the aneurysm and parent artery, respectively, while WSS_{IA} is the average value of WSS in IA. U_{avg} is the spatial range of maximum velocity inside the aneurysm per study and $\dot{\gamma}$ is the range of shear rate inside the aneurysm per study.

a research tool to investigate IA hemodynamics.[82,83] Figure 1(a) shows the trend of using CFD as a research tool in cerebral aneurysm hemodynamics based on Scopus® database. Nevertheless, IA CFD simulations, attempting to provide clinically relevant analyses, had adopted assumptions far from the experience of the earlier *in vitro* works. Now, the highest citations of CFD studies goes to works that have assumed Newtonian blood viscosity[84,85] and laminar flow with no transition to turbulence.[86–88] Figure 1(b) shows a comparison between the citations of early *in vitro* laser measurements encompassing complex physics (i.e. non-Newtonian effects, transition to turbulence) compared with the early CFD works with simplified physical assumptions (i.e. Newtonian viscosity, laminar flow). As a result of such relaxed assumptions in early CFD simulations, the argument favoring the role of high WSS in aneurysm rupture[84,89] challenged an opposing argument correlating low WSS with IA wall disintegration and degeneration leading to rupture.[85,90–92] While in some other CFD studies, low[93] as well as high[94] WSS were controversially correlated to the growth of IA. Several articles[95–99] have highlighted such controversies along the past two decades and discussed the discrepancy of findings, however without providing enough reasoning to their root causes. The recent works of Can et al.,[100] Zhou et al.,[101] and Meng et al.[102] are exemplary endeavors to find coherence among the large IA CFD corpus, however, without definitive and conclusive findings, especially with relevance to IA mechanobiology and clinical applications.

In addition to the attempts of unfolding the physics of IA hemodynamics using CFD, CFD has been a very useful tool in the design, development, and evaluation of endovascular management methods. The term *virtual stenting* has attracted many research groups around the world to empower endovascular management with CFD decision-making tools.[103–106] Adopting simplified flow physics as the mainstream IA CFD works, many research groups have evaluated the embolization efficacy of flow diverters and stents[107,108] and IAs endovascular coiling.[11] In the matter of fact, much of the development in endovascular devices can be attributed to the availability of CFD as an optimization tool for the design, testing and synthesis of such devices. However, the incomplete understanding of complex blood flow dynamics has maintained the concept of such devices with minimal progress along the years. Devices used to treat IAs depend on one concept: flow isolation.[109–112] Stents, coils and flow diverters aim at isolating the aneurysm cavity from the main flow, hence allowing ECs to recover and the vascular wall to heal. In addition to the design complexity of such devices,[113,114] their efficacy depends on IA geometry, morphology, location and other inherent factors of the IA.[115,116] It can safely be argued that a better understanding of IA hemodynamics, and blood dynamics at large, is necessary to radically improve the current design theory of endovascular devices.

Linking hemodynamics to IA mechanobiology

Well-established *in vitro* studies of endothelial cells response to WSS, which is relevant to IA mechanobiology,[117] depend on the Newtonian assumption.[118–120] In such studies, EC cultures are subjected to different levels and regimes of WSS, created by simple Poiseuille-type Newtonian fluid flow,[119,121–123] to investigate the cells response to each WSS level and regime. It has been established, through the vast majority of these studies, that endothelial dysfunction (ED) associated with cerebral aneurysm occurs under WSS regime which can be best classified under *disturbed/turbulent* flow rather than *uniform/laminar* flow.[118,124–126] Chiu and Shien[118] showed that low values of WSS, often associated with *distrubed/turbulent* flow, are associated with long-term ED and remodeling processes similar to those encountered in IA growth. In a comprehensive and extensive meta-analysis, Zhou et al.[127] has also showed that IA rupture is often associated with low WSS values inside the aneurysm. Now, it has been established that EC respond to laminar flow by supressing pro-inflammatory transcription agents and

respond to distrubed (i.e. turbulent-like) flow by upregulating inflammatory and chemotactic mediators.[128] However, these findings have not been reflected on the published CFD studies of IA hemodynamics, as shown in Figure 3(c) and (d) and discussed in the next section, such that only 31% of the studies considered the pulsatile nature of blood flow, while 4% of such studies attempted to explore turbulent-like structure that might exist in IA hemodynamics, as referred to from EC research.

Classification of IA CFD models

CFD models of IA can be generally classified according to the level of complexity to two major categories: ideal and patient-specific models. Figure 2 shows a schematic of the different parameters determining the level of IA CFD model complexity, as explained henceforth. Ideal models are often based on assumed geometry with anatomically relevant dimensions used to study the morphological patterns[129–133] and Neuroendovascular device efficacy.[134,135] Some of the ideal model geometries are actually constructed from averaging of patient-specific dimensions across a specific population to compare the relevance of gender,[136] morphology[137] or complex cases of IA.[138] Patient-specific models are often constructed from DSA images,[139] and then converted to volume meshing suitable for any adequate CFD solver.[41] The discretization of the reconstructed 3D models into computational grid dictates the flow regime and limits the underlying physics in the solution. If the computational grid and time marching scheme are sufficiently accurate, it would be possible to capture

the flow specific physics taking place at higher frequencies[140] such as flow instabilities[141,142] or transition.[143,144] It is also essential to define the solution method, boundary conditions, and the viscosity model to solve the Navier-Stokes equations (NSE) for the blood flow in the aneurysm geometry of interest. There are three main methods for solving NSE numerically for IA blood flow scenarios: the generic finite volume method,[145] adapted finite element methods,[146–148] or the lattice Boltzmann method[149–151] which was recently introduced to the field after success in other numerous applications. The boundary conditions required by any NSE solver for an IA CFD simulation are either steady, pulsatile (i.e. sinusoidal) or Womersley waveform. Steady flow boundary conditions are usually used to provide qualitative assessment of the aneurysm flow field and WSS;[152] however, they are considered to be a form of idealization even if used with patient-specific geometries as they neglect some of the main phenomena in aneurysm hemodynamics and reduce the clinical relevance of the CFD models.[153–155]

As to the blood viscosity models, the majority of IA CFD simulations have adopted Newtonian viscosity assumption when solving the NSE for either steady or pulsatile flows.[10,45,75,84,156,157] Bibliographic meta-analysis from Scopus® database revealed interesting insights about the current paradigm of IA CFD models. The most important aspects of any IA CFD model are the viscosity, transient nature, and flow regime as resolved by the computational grid. Figure 3 summarizes such aspects as revealed by surveying the IA hemodynamics literature. It was found that 47% of published literature studying IA
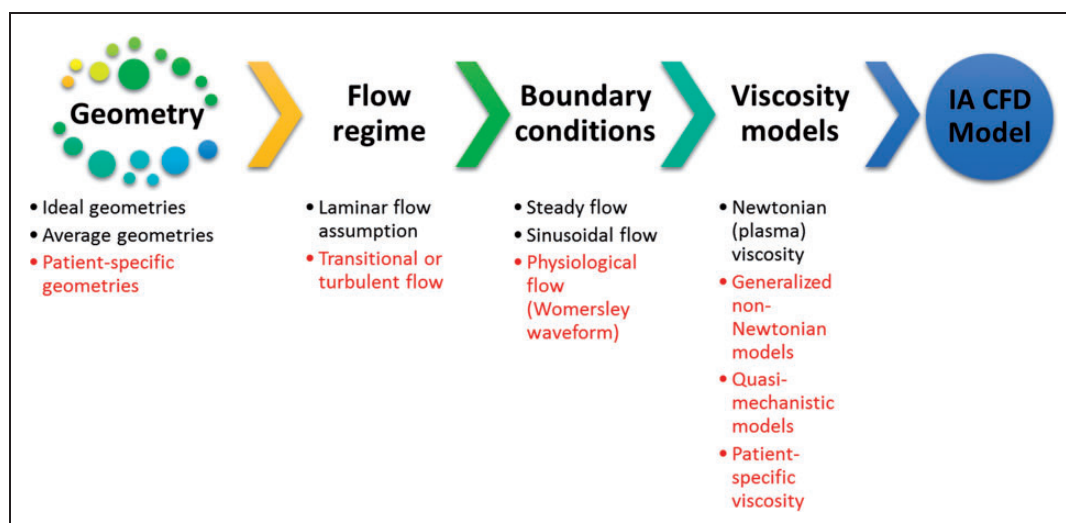
Figure 2. The parameters and assumptions which define the complexity of CFD models. The meshing resolution of the flow domain, boundary conditions as well as the viscosity models and solver numerical settings define the flow physics predicted by the CFD model and whether or not it could model transitional and turbulent features of the flow.
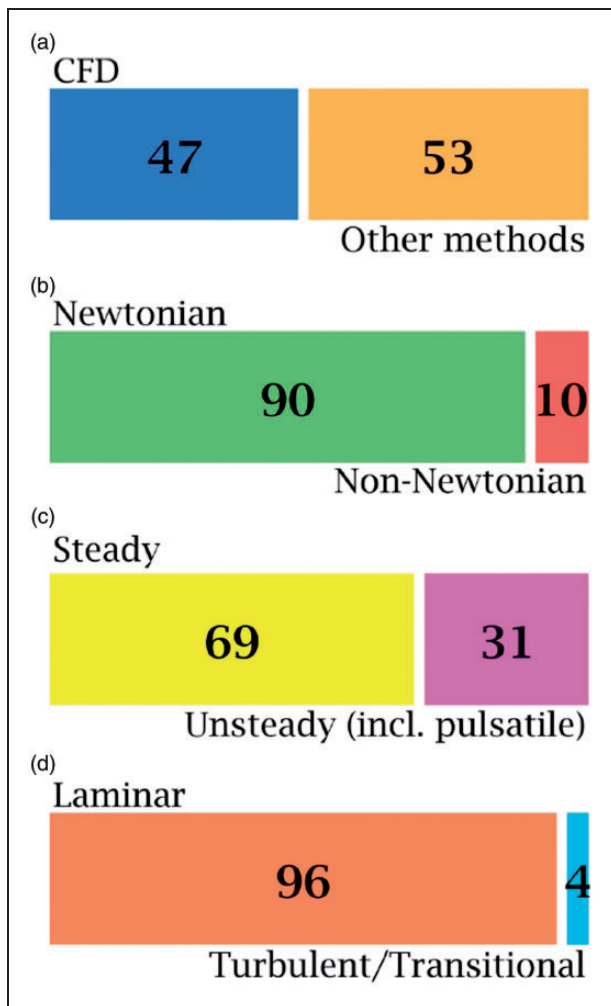
Figure 3. Classification of published studies on intracranial anereurysm hemodynamics with respect to physical assumptions in the CFD models, as revealed by Scopus® bibliographic databases. A total number of 1733 publications was found by searching Scopus® on 14 October 2018. This classification was conducted using sequential searches via Scopus® analytic tools. Classification methodology is explained in the methods section. Articles using CFD as a method of investigation comprised 47% of the literature on aneurysm hemodynamics (a). Of these CFD-based articles, only 10% used the non-Newtonian viscosity assumption to investigate aneurysm hemodynamic features (b), 31% used unsteady and pulsatile models (c) and only 4% investigated turbulence and transition to turbulence (d).

hemodynamics was based on CFD models, while the remaining 53% was shared by *in vitro*, *in vivo*, pathological and other research methods in the field. Only 10% of the published CFD studies to date have considered the non-Newtonian viscosity of blood in modelling intracranial aneurysm hemodynamics. In fact, most of the former studies relied on the assumption that blood viscosity follows a Newtonian behavior in cerebral arteries since the shear rates are presumed to

be higher than the range required for the non-Newtonian properties to become effective.[158–161] Tracing the origins of such assumption was quite difficult, and a considerable number of the highly cited studies in the field have not discussed such assumption in details,[87,162,163] or just refer to the parent artery of the aneurysm to be *large enough* to neglect the non-Newtonian properties of blood.[164,165] While some other studies have arbitrarily used this assumption with some sort of basic physical reasoning,[84,166] some studies simply cite classic publications on erythrocytes[167,168] or plasma[169,170] viscosity to be dominantly Newtonian in *in vitro* measurements, hence, justifying the use of their values in complex *in silico* CFD simulations.

Hemodynamic instabilities and transitional features of aneurysmal flow

In the past few years, some Direct Numerical Simulation (DNS) studies[171–173] were conducted to provide detailed physical insight onto aneurysm hemodynamics. Such studies were performed using the Newtonian viscosity assumption. According to these studies, blood flow in cerebral and intracranial aneurysms exhibits turbulent-like structures and shows subcritical transitional behavior ($Reynolds < 10^3$, $Womersley < 10$) which was shown by monitoring the power spectrum of the velocity time-series at different locations of patient-specific aneurysms. Another study, by the same research group, reported patient-specific CFD simulations of intracranial aneurysm hemodynamics to examine the impact of a non-Newtonian viscosity model in comparison to the effect of solution methods on the results of WSS and Oscillatory Shear Index (OSI).[174] The simulation results, deemed to represent a DNS solution, showed that the impact of non-Newtonian assumption is insignificant in comparison to the impact of solution methods. However, the study has not provided sufficient information on the impact of non-Newtonian viscosity on the turbulence-like structures found in aneurysmal flow as reported previously by the same group of researchers.[171–173] It is well known that non-Newtonian shear thinning fluids, such as blood, are more asymptotically and monotonically stable than Newtonian fluids, such that subcritical transition to turbulence becomes unlikely to take place.[175–177]

The credibility of the DNS results comes from the fact that in DNS, the Navier-Stokes equation is solved to the highest possible resolution of length and time scales.[178,179] Beside its theoretical rigor,[180] DNS has been reproducibly validated in numerous works.[181,182] On the other hand, in commonly used CFD solvers and settings among the community, only the laminar scales

are resolved. Hence, the latter solvers dictate *in priori* simplified physics in the solution. Therefore, and despite their expensive computational cost, DNS solvers have been extensively used for four decades in all areas of fluid dynamics research,[183–185] except in hemodynamics until recently.[186] In DNS settings, the smallest grid cell in the fluid domain should be smaller than the smallest vortex in the flow. The total number of grid cells is often proportional to $Re^{9/4}$ for fully developed turbulent flow.[187] This increases the computational cost of DNS significantly. Rigorous conditions are also applied on the time-marching technique to ensure capturing of the smallest time scale. Vascular blood flow has a multiharmonic pulsatile nature which covers a relatively wide range of length and time scales. In addition, the complex vascular morphology provides perfect conditions to drive the flow towards instability and transition. Therefore, DNS by definition is the best and most reliable method to study vascular blood flow at large, and aneurysm hemodynamics specifically.

It must be noted that the classical theory of hydrodynamic stability has been established to study steady flows subjected to finite perturbations in space and time.[188] The physics underlying transition to turbulence in viscous incompressible flow, as in simple geometries such as straight pipes or under shear conditions, remains in question until today.[189–192] Previous investigations of transition to turbulence in pulsatile pipe flow are limited and have not established a consensus regarding this critical condition.[193–196] It must also be noted that most of such works considered monoharmonic pulsatile flow[196] with very few works that aimed at discussing multiharmonic pulsatile flow which is the nature of the blood flow.[197] Blood flow in IA exhibits several fluid dynamics phenomena depending on the morphology of parent and daughter arteries, as well as the size and location of the IA. Shear layers,[198] precessing vortices,[199,200] jet impingement,[201,202] recirculation and separation zones[203,204] are inherently found in IAs. IA hemodynamics, therefore, are quite different from pulsatile pipe flows investigated in literature for turbulence transition criteria.[194–196,205,206] It is impossible to apply the criteria of laminar-turbulence transition, classically devised for flows in straight pipes, to characterize IA flows. Therefore, fundamental fluid dynamics research is needed to characterize the transition to turbulence in IA flow.

Non-Newtonian properties of intracranial blood flow

Here, we concisely reviewed the previous studies aimed at evaluating the significance of the Newtonian assumption on WSS predictions. It was shown that the use of Newtonian viscosity results in overpredictions of aneurysm wall shear stress (WSS)[207] which could

compromise rupture risk prediction (RRP) efficacy.[208] Frolov et al.[209] conducted *in vitro* comparative study between Newtonian and non-Newtonian blood surrogate fluids to investigate WSS distribution in patient-specific internal carotid artery aneurysm (ICAA) using 1D Laser Doppler Anemometry (LDA) with micrometer-scale spatial resolution. Their results showed that the use of Newtonian fluid over-predicts WSS by 11.7–19.7% at the aneurysm neck and dome, respectively. Hippelheuser et al.[210] investigated the hemodynamics of 26 patient-specific cerebral aneurysm using Newtonian and non-Newtonian (Carreau) viscosity models. Their comparative analysis showed significant differences in time-averaged wall shear stress (TAWSS) between the Newtonian and Carreau models. Such difference impacts the predicted rupture criteria of the aneurysm via CFD. Sano et al.[211] conducted comparative analysis on cerebral aneurysm hemodynamics using CFD. They used patient-specific viscosity data in comparison with the generalized Newtonian assumption. They found up to 25% difference in the normalized wall shear stress (NWSS) between the non-Newtonian and Newtonian simulations. They concluded that any rupture risk criteria, irrespective from aneurysm size, should be significantly affected by the viscosity model used in the CFD simulation. Otani et al.[212] simulated the hemodynamics of a coiled patient-specific cerebral aneurysm using two viscosity models. They used the Carreau-Yasuda non-Newtonian model in comparison with the generalized Newtonian viscosity assumption. They evidently showed that the use of non-Newtonian viscosity model in CFD produces flow structure and hemodynamic parameters that are different from such produced by the Newtonian assumption. More specifically, they identified that the Newtonian assumption underestimates the low shear-rate regions which could possibly skip thrombus formation features in the aneurysm. Moreover, Xiang et al.,[213] Morales et al.,[214] and Owen et al.[215] showed noteworthy differences between the Newtonian and various non-Newtonian blood viscosity models resulting in significant differences in predicted hemodynamics of intracranial aneurysm.

Newtonian vs non-Newtonian WSS calculation

Recently, we[55] provided the first *in vivo* evidence of the large discrepancy between non-Newtonian and Newtonian blood viscosity assumptions in major cerebral arteries from Doppler ultrasound measurements. The following section employs somehow similar methodology,[55] however, with measurements collected from a large pool of radiological studies using different techniques. The measurements and analytical solutions of

the Hagen-Poiseuille and Weissenberg-Rabinowitsch equations are comparatively assessed using statistical paired *t*-tests to evaluate the null hypothesis representing the Newtonian assumption.

The calculations of WSS based on the mathematical model presented in methods section showed considerable variations between the Newtonian and non-Newtonian models, as shown in Figure 4. Different non-Newtonian models over-predict and under-predict Newtonian WSS by values corresponding to 2 and 4 Pa, respectively, as shown in Figure 5. The statistical *t*-test results presented in Table 1 show statistically significant differences between WSS calculation using Newtonian and different non-Newtonian models. In CFD calculations, the Weissenberg-Rabinowitsch (W-R) shear-thinning correction is not applied since the non-Newtonian closure of the shear stress term in Navier-Stokes equation is solved explicitly with the velocity equation. The coupling parameter is therefore the shear rate tensor. Here, the W-R correction is applied in order to ensure that the non-Newtonian calculations of WSS mimic such that from CFD simulations in terms of its proportionality with the Newtonian calculations. The W-R correction has been extensively verified and validated.[216,217] Therefore, the statistical *t*-tests applied here represent meaningful comparison between WSS calculated from Newtonian and non-Newtonian models.

The range of WSS in IAs spans values that correspond to stagnant, creeping, and transitional flows. The order of magnitude of WSS, as depicted in Table 2 by *in vivo* methods, is between 10^{-2} and 10 Pa, depending on numerous factors including size, shape, morphology and location of IA. This range corresponds to shear rates in the order of 10^0 to $10^3\,S^{-1}$. From such *in vivo* measurements, it is clear that blood flow inside the aneurysm manifests the non-Newtonian properties of blood. On the other hand, even in healthy intracranial arteries, the viscous behavior of blood shows considerable variation from the Newtonian simplification. This has been evidently proved from the meta-analysis calculations plotted in Figure 5. The wide range of values of shear rate and corresponding WSS in intracranial arteries clearly proves that the Newtonian assumption is inaccurate both qualitatively and quantitatively. This is quite evident from the hypothesis tests summarized in Table 1. All non-Newtonian models showed differences with the Newtonian model, with the most significant differences attributed to Carreau, Casson and Cross models. Figure 5 shows that Cross and Carreau
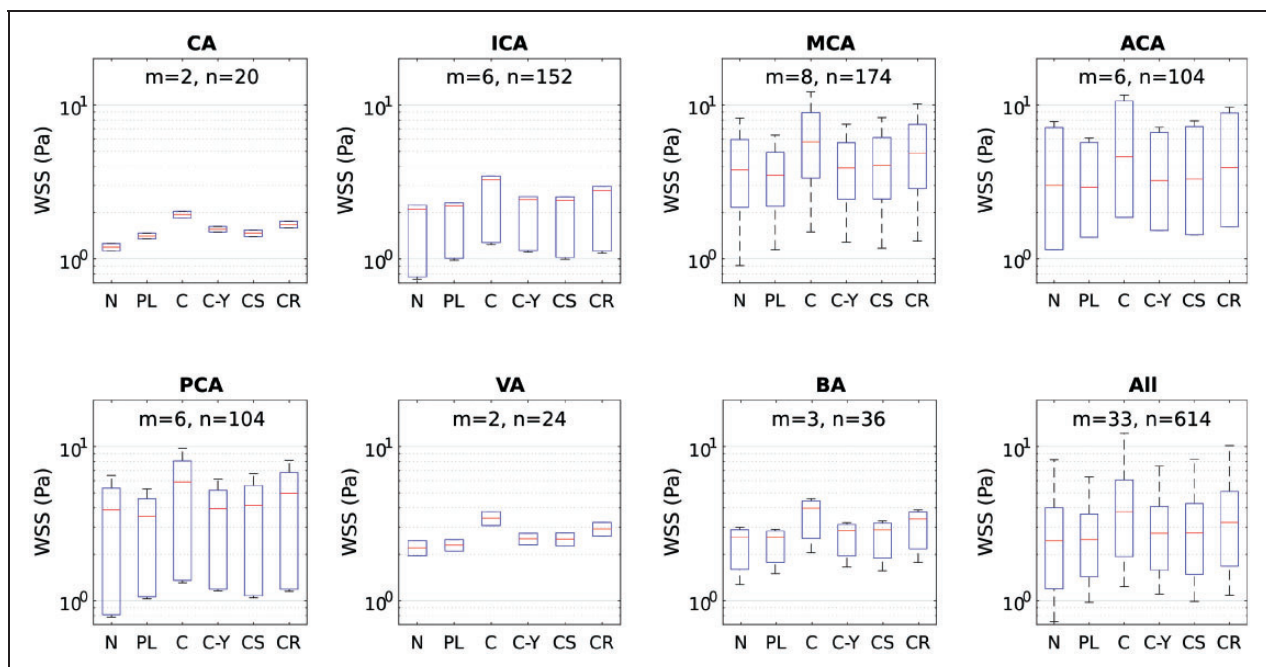

Figure 4. Box plots of WSS as calculated by Newtonian and five different non-Newtonian models in different intracranial arteries which are known for harboring IAs. Box plots were computed using m means for a total of n measurements by artery. The red midline in the box plots represents the median of WSS per artery per model for all studies. Models compared: Newtonian (N), Power-law (PL), Carreau (C), Carreau-Yasuda (C-Y), Casson (CS) and Cross (CR).
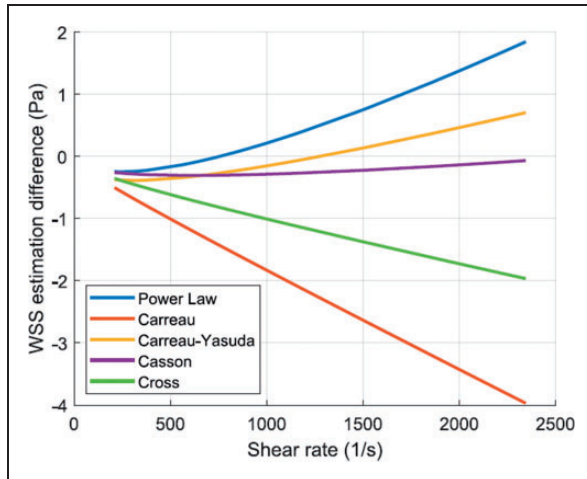
Figure 5. WSS estimation difference ($WSS_N - WSS_{NN}$) as calculated for different non-Newtonian models. Measurements of diameter and flow rate of different intracranial arteries as compiled from the meta-analysis with colors showing different arteries.

models consistently produced WSS that were always higher than the Newtonian assumption. The remaining models produced both negative and positive differences showing varying response to different ranges of shear rate.

Is WSS enough to bridge hemodynamics and aneurysm pathology?

Choosing wall shear stress (WSS) as the discriminant variable to link blood flow (i.e. hemodynamics) to cellular response, hence physiological changes in blood vessels, was an arbitrary choice based on modest physical reasoning. Simply, early works chose WSS since it is the only parameter that depends on the flow (i.e. function of the near-wall shear rate) and shows multicomponent mechanical stress on the wall. Early researches in vascular biomechanics considered blood vessels as elastic or rigid tubes which respond mechanically to blood flow.[218–221] The concept of mechanical response of arteries to blood flow propagated in literature and scientific community in the following decades.[222,223] Following to the discovery of endothelial mechanosensors,[224,225] it was found that endothelial cells respond to flow direction[226,227] and local structures in disturbed flow.[118,228] Flow with inherent vorticity field and vortex structures was found to affect endothelial cells differently than fully developed uniform flow.[118] When any fluid dynamicist thinks of flow structures and directionality, a number of flow field variables arise, excluding WSS. In the supplementary material to this article, we have explained why

WSS is insufficient to justify the response of ECs to flow directionality and local structures in transitional and turbulent flows.

Due to the aforementioned shortcomings of WSS, there has been a recently growing trend to link IA growth and rupture events with other flow variables such as vorticity, coherent structures and turbulence identifying parameters. Valencia et al.[229] investigated the vortex ring structures and recirculation zones in IA models by inspecting the three-dimensional instantaneous velocity vector fields. They identified regimes of flow stability in the IA as function of the aneurysm tilt angle and showed the stabilizing effect of non-Newtonian blood viscosity. The local structures and energy cascade phenomena in IA were also investigated by means of DNS in several studies.[173,191,230] These efforts are promising to link the biology and mechanotransducive responses of ECs to aneurysm pathology. In a pioneering attempt to probe such complex interaction, Varble et al.[231] investigated the vortex structure in 204 patient-specific IAs using high resolution DNS and patient-specific boundary condition waveforms. They evidently shown that IA rupture is significantly correlated with the near-wall vortex structures as expressed in terms of the surface vortex fraction. The outcome of their study highlights a new correlation between aneurysm rupture and higher levels of rotationality and vorticity in the IA flow. This finding is evidently supported by ECs mechanotransduction, where flow disturbance initiates pro-inflammatory EC responses,[66,232] degenerative progress and EC misalignment.[118]

Conclusion: towards next generation IA CFD models

The main challenges facing IA CFD currently have been summarized in the questions proposed in the aim and motivation section. Through the review and meta-analysis, it is evident that tackling such questions is impossible with the present IA CFD models which incorporates inappropriate simplifications, reliance on physically meaningless parameters, and loose computational representation of physiologic blood flow. Next generation IA CFD models must strive towards achiving the following objectives:

- Capture more physics underlying IA hemodynamics
- Provide meaningful parameters to distinguish the pathobiology-hemodynamics interaction in IA genesis, growth and rupture
- Guide EC mechanotransduction studies by providing detailed quantitative and qualitative flow descriptions that can be used to trace biological factors influencing IA

In order to achieve such objectives, next generation IA CFD models must at least incorporate all of the following elements:

I. Patient-specific viscosity and blood flow waveforms
II. Direct numerical simulation or robust large eddy simulation scheme
III. Investigate the flow via one or more of the vector fields (such as vorticity) instead of scalar-tensor field (WSS or OSI)

In the end, modeling a complex biological system as IAs, which involves countless factors from the molecular and cellular levels to the complexities of the interacting blood flow, is never going to be a simple task. Indeed, in such a case some degree of simplification is always warranted, and of course justified. However, over-simplification in the modeling would eventually hinder us from capturing phenomena that could correlate the physics with the biology and ultimately enhance our understanding of the pathology of IAs.

Declaration of conflicting interests

The author(s) declared no potential conflicts of interest with respect to the research, authorship, and/or publication of this article.

Authors' contributions

KMS conceived and designed the study, contributed data, developed the mathematical models and wrote the paper. SR contributed data and wrote the paper. ST was responsible for the Software, statistics and visualization. KN, TH and TT critically revised the manuscript. MO was involved in funding acquisition, project management, and critical review of the paper. All authors approved the final version of the manuscript.

ORCID iDs

Sherif Rashad https://orcid.org/0000-0002-4511-6360
Simon Tupin https://orcid.org/0000-0003-0982-8210

Supplemental material

Supplemental material for this paper can be found at the journal website: http://journals.sagepub.com/home/jcb

References

1. Amenta PS, Yadla S, Campbell PG, et al. Analysis of nonmodifiable risk factors for intracranial aneurysm rupture in a large, retrospective cohort. *Neurosurgery* 2012; 70: 693–699; discussion 699–701.
2. Rashad S, Hassan T, Aziz W, et al. Carotid artery occlusion for the treatment of symptomatic giant carotid aneurysms: a proposal of classification and surgical protocol. *Neurosurg Review* 2014; 37: 501–511; discussion 511.
3. Algra AM, Lindgren A, Vergouwen MDI, et al. Procedural clinical complications, case-fatality risks, and risk factors in endovascular and neurosurgical treatment of unruptured intracranial aneurysms: a systematic review and meta-analysis. *JAMA Neurology* 2019; 76(3): 282–293.
4. Brisman JL, Song JK and Newell DW. Cerebral aneurysms. *New Engl J Med* 2006; 355: 928–939.
5. Wiebers DO, Whisnant JP, Huston J 3rd, et al. Unruptured intracranial aneurysms: natural history, clinical outcome, and risks of surgical and endovascular treatment. *Lancet (London, England)* 2003; 362: 103–110.
6. Cornelissen BM, Schneiders JJ, Potters WV, et al. Hemodynamic differences in intracranial aneurysms before and after rupture. *AJNR Am J Neuroradiol* 2015; 36: 1927–1933.
7. Chien A and Sayre J. Morphologic and hemodynamic risk factors in ruptured aneurysms imaged before and after rupture. *AJNR Am J Neuroradiol* 2014; 35: 2130–2135.
8. Sugiyama SI, Endo H, Omodaka S, et al. Daughter sac formation related to blood inflow jet in an intracranial aneurysm. *World Neurosurg* 2016; 96: 396–402.
9. Vlak MH, Algra A, Brandenburg R, et al. Prevalence of unruptured intracranial aneurysms, with emphasis on sex, age, comorbidity, country, and time period: a systematic review and meta-analysis. *Lancet Neurol* 2011; 10: 626–636.
10. Rashad S, Sugiyama SI, Niizuma K, et al. Impact of bifurcation angle and inflow coefficient on the rupture risk of bifurcation type basilar artery tip aneurysms. *J Neurosurg* 2018; 128: 723–730.
11. Sugiyama S, Niizuma K, Sato K, et al. Blood flow into basilar tip aneurysms: a predictor for recanalization after coil embolization. *Stroke* 2016; 47: 2541–2547.
12. Wiebers DO, Torner JC and Meissner I. Impact of unruptured intracranial aneurysms on public health in the United States. *Stroke* 1992; 23: 1416–1419.
13. Baratchi S, Khoshmanesh K, Woodman OL, et al. Molecular sensors of blood flow in endothelial cells. *Trends Mol Med* 2017; 23(9): 850–868.
14. Tarbell JM, Simon SI and Curry FR. Mechanosensing at the vascular interface. *Annu Rev Biomed Eng* 2014; 16: 505–532.
15. Chiu J-J and Chien S. Effects of disturbed flow on vascular endothelium: pathophysiological basis and clinical perspectives. *Physiol Rev* 2011; 91: 327–387.
16. Zhang Q, Meng Z, Zhang Y, et al. Phantom-based experimental validation of fast virtual deployment of

self-expandable stents for cerebral aneurysms. *BioMed Eng Online* 2016; 28; 15(Suppl 2): 125. DOI: 10.1186/s12938-016-0250-6.

17. Hergenreider E, Heydt S, Treguer K, et al. Atheroprotective communication between endothelial cells and smooth muscle cells through miRNAs. *Nature Cell Biol* 2012; 14: 249–256.

18. Humphrey JD. Vascular adaptation and mechanical homeostasis at tissue, cellular, and sub-cellular levels. *Cell Biochem Biophys* 2008; 50: 53–78.

19. Dolan JM, Kolega J and Meng H. High wall shear stress and spatial gradients in vascular pathology: a review. *Ann Biomed Eng* 2013; 41: 1411–1427.

20. Cebral J, Ollikainen E, Chung BJ, et al. Flow conditions in the intracranial aneurysm lumen are associated with inflammation and degenerative changes of the aneurysm wall. *AJNR Am J Neuroradiol* 2017; 38: 119–126.

21. Davies PF, Remuzzi A, Gordon EJ, et al. Turbulent fluid shear stress induces vascular endothelial cell turnover in vitro. *Proc Natl Acad Sci U S A* 1986; 83: 2114–2117.

22. Miao H, Hu YL, Shiu YT, et al. Effects of flow patterns on the localization and expression of VE-cadherin at vascular endothelial cell junctions: in vivo and in vitro investigations. *J Vasc Res* 2005; 42: 77–89.

23. Hosaka K and Hoh BL. Inflammation and cerebral aneurysms. *Translat Stroke Res* 2014; 5: 190–198.

24. Korkmaz E, Kleinloog R, Verweij BH, et al. Comparative ultrastructural and stereological analyses of unruptured and ruptured saccular intracranial aneurysms. *J Neuropathol Exp Neurol* 2017; 76: 908–916.

25. Robertson AM, Duan X, Aziz KM, et al. Diversity in the strength and structure of unruptured cerebral aneurysms. *Ann Biomed Eng* 2015; 43: 1502–1515.

26. Roach MR, Scott S and Ferguson GG. The hemodynamic importance of the geometry of bifurcations in the circle of willis (Glass model studies). *Stroke* 1972; 3: 255–267.

27. Ferguson GG. Physical factors in the initiation, growth, and rupture of human intracranial saccular aneurysms. *J Neurosurg* 1972; 37: 666–677.

28. Ferguson GG. Turbulence in human intracranial saccular aneurysms. *J Neurosurg* 1970; 33: 485–497.

29. Steiger HJ and Reulen HJ. Low frequency flow fluctuations in saccular aneurysms. *Acta neurochirurgica* 1986; 83: 131–137.

30. Liepsch DW, Steiger HJ, Poll A, et al. Hemodynamic stress in lateral saccular aneurysms. *Biorheology* 1987; 24: 689–710.

31. Gonzalez CF, Cho YI, Ortega HV, et al. Intracranial aneurysms: flow analysis of their origin and progression. *Am J Neuroradiol* 1992; 13: 181–188.

32. Kim C, Cervós-Navarro J, Pätzold C, et al. In vivo study of flow pattern at human carotid bifurcation with regard to aneurysm development. *Acta Neurochirurgica* 1992; 115: 112–117.

33. Burleson AC and Turitto VT. Identification of quantifiable hemodynamic factors in the assessment of cerebral aneurysm behavior: on behalf of the subcommittee on biorheology of the scientific and standardization committee of the ISTH. *Thrombosis Haemostasis* 1996; 76: 118–123.

34. Steiger HJ, Liepsch DW, Poll A, et al. Hemodynamic stress in terminal saccular aneurysms: a laser-Doppler study. *Heart Vessels* 1988; 4: 162–169.

35. Liepsch D, Poll A, Steiger HJ, et al. Laser-Doppler-velocity-measurements in lateral aneurysms. In: *In 1987 Biomechanics Symposium: presented at the 1987 ASME Applied Mechanics, Bioengineering, and Fluids Engineering Conference*, Cincinnati, Ohio, June 14–17, 1987, Vol. 84, p.33. American Society of Mechanical Engineers, 1987.

36. Tognetti F, Limoni P and Testa C. Aneurysm growth and hemodynamic stress. *Surg Neurol* 1983; 20: 74–78.

37. Tognetti F, Andreoli A and Testa C. Hemodynamic mechanism in the angiographic disappearance of ruptured cerebral aneurysm. *Surg Neurol* 1984; 22: 412–414.

38. Steiger HJ, Poll A, Liepsch D, et al. Haemodynamic stress in lateral saccular aneurysms – an experimental study. *Acta Neurochirurgica* 1987; 86: 98–105.

39. Steiger HJ, Poll A, Liepsch DW, et al. Haemodynamic stress in terminal aneurysms. *Acta Neurochirurgica* 1988; 93: 18–23.

40. Steiger HJ, Aaslid R, Keller S, et al. Growth of aneurysms can be understood as passive yield to blood pressure – an experimental study. *Acta Neurochirurgica* 1989; 100: 74–78.

41. Hassan T, Timofeev EV, Saito T, et al. Computational replicas: anatomic reconstructions of cerebral vessels as volume numerical grids at three-dimensional angiography. *Am J Neuroradiol* 2004; 25: 1356–1365.

42. Sugiyama SI, Endo H, Omodaka S, et al. Daughter sac formation related to blood inflow jet in an intracranial aneurysm. *World Neurosurg* 2016; 96: 396–402.

43. Sugiyama SI, Niizuma K, Nakayama T, et al. Relative residence time prolongation in intracranial aneurysms: a possible association with atherosclerosis. *Neurosurgery* 2013; 73: 767–776.

44. Lasheras JC. The biomechanics of arterial aneurysms. *Annual Rev Fluid Mech* 2007; 39: 293–319.

45. Sforza DM, Putman CM and Cebral JR. Hemodynamics of cerebral aneurysms. *Ann Rev Fluid Mech* 2009; 41: 91–107.

46. Hassan T, Timofeev EV, Ezura M, et al. Hemodynamic analysis of an adult vein of Galen aneurysm malformation by use of 3D image-based computational fluid dynamics. *Am J Neuroradiol* 2003; 24: 1075–1082.

47. Hassan T, Timofeev EV, Saito T, et al A proposed parent vessel geometry—based categorization of saccular intracranial aneurysms: computational flow dynamics analysis of the risk factors for lesion rupture. *J Neurosurg* 2005; 103: 662.

48. Chatziprodromou I, Tricoli A, Poulikakos D, et al. Haemodynamics and wall remodelling of a growing cerebral aneurysm: a computational model. *J Biomech* 2007; 40: 412–426.

49. Cardamone L and Humphrey JD. Arterial growth and remodelling is driven by hemodynamics. *Model Simulat Appl* 2012; 5: 187–203.

50. Meng H, Feng Y, Woodward SH, et al. Mathematical model of the rupture mechanism of intracranial saccular

aneurysms through daughter aneurysm formation and growth. *Neurol Res* 2005; 27: 459–465.

51. Hassan T, Ezura M, Timofeev EV, et al. Computational simulation of therapeutic parent artery occlusion to treat giant vertebrobasilar aneurysm. *Am J Neuroradiol* 2004; 25: 63–68.

52. Donaldson CJ, Lao KH and Zeng L. The salient role of microRNAs in atherogenesis. *J Mol Cellular Cardiol* 2018; 122: 98–113.

53. Meng H, Tutino VM, Xiang J, et al. High WSS or low WSS? Complex interactions of hemodynamics with intracranial aneurysm initiation, growth, and rupture: toward a unifying hypothesis. *AJNR Am J Neuroradiol* 2014; 35: 1254–1262.

54. Zhou G, Zhu Y, Yin Y, et al. Association of wall shear stress with intracranial aneurysm rupture: systematic review and meta-analysis. *Scientific Rep* 2017; 7: 5331.

55. Saqr KM, Mansour O, Tupin S, et al. Evidence for non-Newtonian behavior of intracranial blood flow from Doppler ultrasonography measurements. *Med Biol Eng Comput* 2018; 57(5): 1029–1036.

56. Saqr KM. Wall shear stress in the Navier-Stokes equation: a commentary. *Comput Biol Med* 2019; 106: 82–83.

57. Murray CD. The physiological principle of minimum work applied to the angle of branching of arteries. *J General Physiol* 1926; 9: 835–841.

58. Ingebrigtsen T, Morgan MK, Faulder K, et al. Bifurcation geometry and the presence of cerebral artery aneurysms. *J Neurosurg* 2004; 101: 108–113.

59. Reneman RS and Hoeks APG. Wall shear stress as measured in vivo: consequences for the design of the arterial system. *Med Biol Eng Comput* 2008; 46: 499–507.

60. Beare RJ, Das G, Ren M, et al. Does the principle of minimum work apply at the carotid bifurcation: a retrospective cohort study. *BMC Medical Imaging* 2011; 11: 17.

61. Chnafa C, Bouillot P, Brina O, et al. Errors in power-law estimations of inflow rates for intracranial aneurysm CFD. *J Biomech* 2018; 80: 159–165.

62. Nixon AM, Gunel M and Sumpio BE. The critical role of hemodynamics in the development of cerebral vascular disease: a review. *J Neurosurg* 2010; 112: 1240–1253.

63. Diehl RR, Linden D, Lücke D, et al. Phase relationship between cerebral blood flow velocity and blood pressure a clinical test of autoregulation. *Stroke* 1995; 26: 1801–1804.

64. Reinhard M, Wehrle-Wieland E, Grabiak D, et al. Oscillatory cerebral hemodynamics-the macro- vs. microvascular level. *J Neurol Sci* 2006; 250: 103–109.

65. Basarab MA, Basarab DA, Konnova NS, et al. Analysis of chaotic and noise processes in a fluctuating blood flow using the Allan variance technique. *Clin Hemorheology Microcirculat* 2016; 64: 921–930.

66. Li YSJ, Haga JH and Chien S. Molecular basis of the effects of shear stress on vascular endothelial cells. *J Biomech* 2005; 38: 1949–1971.

67. Moher D, Shamseer L, Clarke M, et al. Preferred reporting items for systematic review and meta-analysis protocols (PRISMA-P) 2015 statement. *Systematic Rev* 2015; 4: 1.

68. Westerhof N, Stergiopulos N and Noble MI. *Snapshots of hemodynamics: an aid for clinical research and graduate education*. New York, NY: Springer Science & Business Media, 2010.

69. Hoskins PR, Lawford PV and Doyle BJ. *Cardiovascular biomechanics*. New York, NY: Springer International Publishing, 2017.

70. Drazin PG, Riley N, Society LM, et al. *The Navier-Stokes equations: a classification of flows and exact solutions*. Cambridge: Cambridge University Press, 2006.

71. Macosko CW. *Rheology: principles, measurements, and applications*. VCH, 1994.

72. Galdi GP, Rannacher R, Robertson AM, et al. *Hemodynamical flows: modeling, analysis and simulation*. Basel: Birkhäuser, 2008.

73. Shibeshi SS and Collins WE. The rheology of blood flow in a branched arterial system. *Appl Rheology (Lappersdorf, Germany: Online)* 2005; 15: 398–405.

74. Carreau PJ. Rheological equations from molecular network theories. *Transact Soc Rheol* 1972; 16: 99–127.

75. Campo-Deano L, Oliveira MSN and Pinho FT. A review of computational hemodynamics in middle cerebral aneurysms and rheological models for blood flow. *Appl Mech Rev* 2015; 67.

76. Schirmer CM and Malek AM. Critical influence of framing coil orientation on intra-aneurysmal and neck region hemodynamics in a sidewall aneurysm model. *Neurosurgery* 2010; 67: 1692–1702.

77. Gijsen FJH, van de Vosse FN and Janssen JD. The influence of the non-Newtonian properties of blood on the flow in large arteries: steady flow in a carotid bifurcation model. *J Biomech* 1999; 32: 601–608.

78. Bernabeu MO, Nash RW, Groen D, et al. Impact of blood rheology on wall shear stress in a model of the middle cerebral artery. *Interface focus* 2013; 3: 20120094.

79. Boyd J, Buick JM and Green S. Analysis of the Casson and Carreau-Yasuda non-Newtonian blood models in steady and oscillatory flows using the lattice Boltzmann method. *Phys Fluids* 2007; 19: 093103.

80. Kim S, Namgung B, Ong PK, et al. Determination of rheological properties of whole blood with a scanning capillary-tube rheometer using constitutive models. *J Mech Sci Technol* 2009; 23: 1718–1726.

81. Bodnár T, Sequeira A and Pirkl L. Numerical simulations of blood flow in a stenosed vessel under different flow rates using a generalized Oldroyd-B model. *AIP Conference Proc* 2009; 1168: 645–648.

82. Burleson AC, Strother CM and Turitto VT. Computer modeling of intracranial saccular and lateral aneurysms for the study of their hemodynamics. *Neurosurgery* 1995; 37: 774–784.

83. Ortega HV. Predicting cerebral aneurysms with CFD. *Mech Eng* 1997; 119: 76–77.

84. Cebral JR, Castro MA, Burgess JE, et al. Characterization of cerebral aneurysms for assessing risk of rupture by using patient-specific computational hemodynamics models. *Am J Neuroradiol* 2005; 26: 2550–2559.

85. Shojima M, Oshima M, Takagi K, et al. Magnitude and role of wall shear stress on cerebral aneurysm:

computational fluid dynamic study of 20 middle cerebral artery aneurysms. *Stroke* 2004; 35: 2500–2505.

86. Cebral JR, Castro MA and Putman CM. A study of the hemodynamics of anterior communicating artery aneurysms. In: *Progress in biomedical optics and imaging – proceedings of SPIE*, 11–16 February 2006, San Diego, California, United States.

87. Cebral JR, Mut F, Weir J, et al. Quantitative characterization of the hemodynamic environment in ruptured and unruptured brain aneurysms. *AJNR Am J Neuroradiol* 2011; 32: 145–151.

88. Castro MA, Putman CM and Cebral JR. Computational fluid dynamics modeling of intracranial aneurysms: effects of parent artery segmentation on intra-aneurysmal hemodynamics. *Am J Neuroradiol* 2006; 27: 1703–1709.

89. Cebral JR, Castro MA, Millan D, et al. Pilot clinical study of aneurysm rupture using image-based computational fluid dynamics models. In: *Progress in biomedical optics and imaging – proceedings of SPIE*, 12–17 February 2005, San Diego, California, United States, pp.245–256.

90. Goubergrits L, Schaller J, Kertzscher U, et al. Statistical wall shear stress maps of ruptured and unruptured middle cerebral artery aneurysms. *J Royal Society Interface* 2012; 9: 677–688.

91. Omodaka S, Sugiyama SI, Inoue T, et al. Local hemodynamics at the rupture point of cerebral aneurysms determined by computational fluid dynamics analysis. *Cerebrovasc Dis* 2012; 34: 121–129.

92. Rashad S, Sugiyama SI, Niizuma K, et al. Impact of bifurcation angle and inflow coefficient on the rupture risk of bifurcation type basilar artery tip aneurysms. *J Neurosurg* 2018; 128: 723–730.

93. Boussel L, Rayz V, McCulloch C, et al. Aneurysm growth occurs at region of low wall shear stress: Patient-specific correlation of hemodynamics and growth in a longitudinal study. *Stroke* 2008; 39: 2997–3002.

94. Sugiyama SI, Meng H, Funamoto K, et al. Hemodynamic analysis of growing intracranial aneurysms arising from a posterior inferior cerebellar artery. *World Neurosurg* 2012; 78: 462–468.

95. Xiang J, Tutino VM, Snyder KV, et al. CFD: Computational fluid dynamics or confounding factor dissemination? the role of hemodynamics in intracranial aneurysm rupture risk assessment. *Am J Neuroradiol* 2014; 35: 1849–1857.

96. Fiorella D, Sadasivan C, Woo HH, et al. Regarding "aneurysm rupture following treatment with flow-diverting stents: Computational hemodynamics analysis of treatment". *Am J Neuroradiol* 2011; 32: E95–E97.

97. Robertson AM and Watton PN. Computational fluid dynamics in aneurysm research: critical. *Am J Neuroradiol* 2012; 33: 992–995.

98. Taylor CA and Humphrey JD. Open problems in computational vascular biomechanics: hemodynamics and arterial wall mechanics. *Comput Meth Appl Mech Eng* 2009; 198: 3514–3523.

99. Humphrey JD and Taylor CA. Intracranial and abdominal aortic aneurysms: similarities, differences, and need for a new class of computational models. *Ann Rev Biomed Eng* 2008; 10: 221–246.

100. Can A and Du R. Association of hemodynamic factors with intracranial aneurysm formation and rupture: systematic review and meta-analysis. *Neurosurgery* 2016; 78: 510–519.

101. Zhou G, Zhu Y, Yin Y, et al. Association of wall shear stress with intracranial aneurysm rupture: systematic review and meta-analysis. *Scientific Reports* 2017; 7: 5331.

102. Meng H, Tutino VM, Xiang J, et al. High WSS or Low WSS? Complex interactions of hemodynamics with intracranial aneurysm initiation, growth, and rupture: toward a unifying hypothesis. *Am J Neuroradiol* 2014; 35: 1254–1262.

103. Janiga G, Daróczy L, Berg P, et al. An automatic CFD-based flow diverter optimization principle for patient-specific intracranial aneurysms. *J Biomech* 2015; 48: 3846–3852.

104. Ma D, Dumont TM, Kosukegawa H, et al. High fidelity virtual stenting (HiFiVS) for intracranial aneurysm flow diversion: In vitro and in silico. *Ann Biomed Eng* 2013; 41: 2143–2156.

105. Paliwal N, Yu H, Xu J, et al. Virtual stenting workflow with vessel-specific initialization and adaptive expansion for neurovascular stents and flow diverters. *Comput Meth Biomech Biomed Eng* 2016; 19: 1423–1431.

106. Song Y, Choe J, Liu H, et al. Virtual stenting of intracranial aneurysms: application of hemodynamic modification analysis. *Acta Radiologica* 2016; 57: 992–994.

107. Shobayashi Y, Tateshima S, Kakizaki R, et al. Intra-aneurysmal hemodynamic alterations by a self-expandable intracranial stent and flow diversion stent: high intra-aneurysmal pressure remains regardless of flow velocity reduction. *J Neurointerventional Surg* 2013; 5: iii38–iii42.

108. Zhang Y, Chong W and Qian Y. Investigation of intracranial aneurysm hemodynamics following flow diverter stent treatment. *Med Eng Phys* 2013; 35: 608–615.

109. Dholakia R, Sadasivan C, Fiorella DJ, et al. Hemodynamics of flow diverters. *J Biomech Eng* 2017; 139: 139–140.

110. Alderazi YJ, Shastri D, Kass-Hout T, et al. Flow diverters for intracranial aneurysms. *Stroke Res Treat* 2014; 2014.

111. Tse MMY, Yan B, Dowling RJ, et al. Current status of pipeline embolization device in the treatment of intracranial aneurysms: a review. *World Neurosurg* 2013; 80: 829–835.

112. Dorn F, Niedermeyer F, Balasso A, et al. The effect of stents on intra-aneurysmal hemodynamics: in vitro evaluation of a pulsatile sidewall aneurysm using laser Doppler anemometry. *Neuroradiology* 2011; 53: 267–272.

113. Jeong W, Han MH and Rhee K. Effects of framing coil shape, orientation, and thickness on intra-aneurysmal flow. *Med Biol Eng Comput* 2013; 51: 981–990.

114. Baráth K, Cassot F, Fasel JHD, et al. Influence of stent properties on the alteration of cerebral intra-aneurysmal

haemodynamics: flow quantification in elastic sidewall aneurysm models. *Neurol Res* 2005; 27: S120–S128.

115. Wu YF, Yang PF, Shen J, et al. A comparison of the hemodynamic effects of flow diverters on wide-necked and narrow-necked cerebral aneurysms. *J Clin Neurosci* 2012; 19: 1520–1524.

116. Mut F, Ruijters D, Babic D, et al. Effects of changing physiologic conditions on the in vivo quantification of hemodynamic variables in cerebral aneurysms treated with flow diverting devices. *Int J Num Meth Biomed Eng* 2014; 30: 135–142.

117. Dolan JM, Meng H, Sim FJ, et al. Differential gene expression by endothelial cells under positive and negative streamwise gradients of high wall shear stress. *Am J Physiol – Cell Physiol* 2013; 305: C854–C866.

118. Chiu JJ and Chien S. Effects of disturbed flow on vascular endothelium: pathophysiological basis and clinical perspectives. *Physiol Rev* 2011; 91: 327–387.

119. Avari H, Savory E and Rogers KA. An in vitro hemodynamic flow system to study the effects of quantified shear stresses on endothelial cells. *Cardiovasc Eng Technol* 2016; 7: 44–57.

120. Dolan JM, Sim FJ, Meng H, et al. Endothelial cells express a unique transcriptional profile under very high wall shear stress known to induce expansive arterial remodeling. *Am J Physiol Cell Physiol* 2012; 302: C1109–C1118.

121. Taba Y, Sasaguri T, Miyagi M, et al. Fluid shear stress induces lipocalin-type prostaglandin D2 synthase expression in vascular endothelial cells. *Circulat Res* 2000; 86: 967–973.

122. Partridge J, Carlsen H, Enesa K, et al. Laminar shear stress acts as a switch to regulate divergent functions of NF-κB in endothelial cells. *Faseb J* 2007; 21: 3553–3561.

123. Dolan JM, Meng H, Singh S, et al. High fluid shear stress and spatial shear stress gradients affect endothelial proliferation, survival, and alignment. *Ann Biomed Eng* 2011; 39: 1620–1631.

124. Chalouhi N, Hoh BL and Hasan D. Review of cerebral aneurysm formation, growth, and rupture. *Stroke* 2013; 44: 3613–3622.

125. Fukuda S and Shimogonya Y. The role of hemodynamic factors on the development, enlargement, and rupture of cerebral aneurysms: a combination of computational fluid dynamics analysis and an animal model study. *Japanese J Neurosurg* 2014; 23: 661–666.

126. Turjman AS, Turjman F and Edelman ER. Role of fluid dynamics and inflammation in intracranial aneurysm formation. *Circulation* 2014; 129: 373.

127. Zhou G, Zhu Y, Yin Y, et al. Association of wall shear stress with intracranial aneurysm rupture: systematic review and meta-analysis. *Sci Rep* 2017; 7: 5331.

128. Hudson JS, Hoyne DS and Hasan DM. Inflammation and human cerebral aneurysms: current and future treatment prospects. *Future Neurol* 2013; 8: 663–676.

129. Bouillot P, Brina O, Ouared R, et al. Multi-time-lag PIV analysis of steady and pulsatile flows in a sidewall aneurysm. *Experiment Fluids* 2014; 55: 1746–1757.

130. Farnoush A, Avolio A and Qian Y. Effect of bifurcation angle configuration and ratio of daughter diameters on

hemodynamics of bifurcation aneurysms. *Am J Neuroradiol* 2013; 34: 391–396.

131. Rafat M, Stone HA, Auguste DT, et al. Impact of diversity of morphological characteristics and Reynolds number on local hemodynamics in basilar aneurysms. *AIChE J* 2018; 64: 2792–2802.

132. Baharoglu MI, Schirmer CM, Hoit DA, et al. Aneurysm inflow-angle as a discriminant for rupture in sidewall cerebral aneurysms: morphometric and computational fluid dynamic analysis. *Stroke* 2010; 41: 1423–1430.

133. Ford MD, Lee SW, Lownie SP, et al. On the effect of parent-aneurysm angle on flow patterns in basilar tip aneurysms: towards a surrogate geometric marker of intra-aneurismal hemodynamics. *J Biomech* 2008; 41: 241–248.

134. Wang C, Tian Z, Liu J, et al. Hemodynamic alterations for various stent configurations in idealized wide-neck basilar tip aneurysm. *J Med Biol Eng* 2016; 36: 379–385.

135. Otani T, Nakamura M, Fujinaka T, et al. Computational fluid dynamics of blood flow in coil-embolized aneurysms: effect of packing density on flow stagnation in an idealized geometry. *Med Biol Eng Comput* 2013; 51: 901–910.

136. Lindekleiv HM, Valen-Sendstad K, Morgan MK, et al. Sex differences in intracranial arterial bifurcations. *Gender Med* 2010; 7: 149–155.

137. Retarekar R, Ramachandran M, Berkowitz B, et al. Stratification of a population of intracranial aneurysms using blood flow metrics. *Comput Meth Biomech Biomed Eng* 2015; 18: 1072–1082.

138. Castro MA, Peloc NL, Putman CM, et al. Computational hemodynamic study of intracranial aneurysms coexistent with proximal artery stenosis. In: *Progress in biomedical optics and imaging – Proceedings of SPIE*, 4–9 February 2012, San Diego, California, United States.

139. Berg P, Saalfeld S, Voß S, et al. Does the DSA reconstruction kernel affect hemodynamic predictions in intracranial aneurysms? An analysis of geometry and blood flow variations. *J Neurointerventional Surg* 2018; 10: 290–296.

140. Jain K, Roller S and Mardal KA. Transitional flow in intracranial aneurysms – a space and time refinement study below the Kolmogorov scales using Lattice Boltzmann Method. *Comput Fluids* 2016; 127: 36–46.

141. Xu L, Liang F, Gu L, et al. Flow instability detected in ruptured versus unruptured cerebral aneurysms at the internal carotid artery. *J Biomech* 2018; 72: 187–199.

142. Varble N, Xiang J, Lin N, et al. Flow instability detected by high-resolution computational fluid dynamics in fifty-six middle cerebral artery aneurysms. *J Biomech Eng* 2016; 138(6): 061009.

143. Poelma C, Watton PN and Ventikos Y. Transitional flow in aneurysms and the computation of haemodynamic parameters. *J Royal Society Interface* 2015; 12(105): 20141394.

144. Yagi T, Sato A, Shinke M, et al. Experimental insights into flow impingement in cerebral aneurysm by stereoscopic particle image velocimetry: transition from a

laminar regime. *J Royal Soc Interface* 2013; 10(82): 20121031.

145. Otani T, Ii S, Fujinaka T, et al. Blood flow analysis in patient-specific cerebral aneurysm models with realistic configuration of embolized coils. In: *IFMBE Proceedings* 2014 4th–7th December 2013, Singapore, pp.343-346.

146. Babiker MH, Chong B, Gonzalez LF, et al. Finite element modeling of embolic coil deployment: Multifactor characterization of treatment effects on cerebral aneurysm hemodynamics. *J Biomech* 2013; 46: 2809–2816.

147. Oshima M, Torii R, Kobayashi T, et al. Finite element simulation of blood flow in the cerebral artery. *Comput Meth Appl Mech Eng* 2001; 191: 661–671.

148. Foutrakis GN, Yonas H and Sclabassi RJ. Finite element methods in the simulation and analysis of intracranial blood flow. *Neurol Res* 1997; 19: 174–186.

149. Sun SR, Huang CS, Wang L, et al. Stent effects on hemodynamics of cerebral aneurysm by non-uniform lattice Boltzmann method. *Yiyong Shengwu Lixue/J Med Biomech* 2015; 30: 104–110.

150. Huang C, Shi B, Guo Z, et al. Multi-GPU based lattice boltzmann method for hemodynamic simulation in patient-specific cerebral aneurysm. *Commun Computat Phys* 2015; 17: 960–974.

151. Shi Y, Tang GH and Tao WQ. Lattice Boltzmann study ofnon-newtonian blood flow in mother and daughter aneurysm and a novel stent treatment. *Adv Appl Math Mech* 2014; 6: 165–178.

152. Geers AJ, Larrabide I, Morales HG, et al. Approximating hemodynamics of cerebral aneurysms with steady flow simulations. *J Biomech* 2014; 47: 178–185.

153. Le TB, Troolin DR, Amatya D, et al. Vortex phenomena in sidewall aneurysm hemodynamics: experiment and numerical simulation. *Ann Biomed Eng* 2013; 41: 2157–2170.

154. Venugopal P, Valentino D, Schmitt H, et al. Sensitivity of patient-specific numerical simulation of cerebal aneurysm hemodynamics to inflow boundary conditions. *J Neurosurg* 2007; 106: 1051–1060.

155. Pereira VM, Brina O, Marcos Gonzales A, et al. Evaluation of the influence of inlet boundary conditions on computational fluid dynamics for intracranial aneurysms: a virtual experiment. *J Biomech* 2013; 46: 1531–1539.

156. Hoi Y, Meng H, Woodward SH, et al. Effects of arterial geometry on aneurysm growth: three-dimensional computational fluid dynamics study. *J Neurosurg* 2004; 101: 676–681.

157. Meng H, Wang Z, Hoi Y, et al. Complex hemodynamics at the apex of an arterial bifurcation induces vascular remodeling resembling cerebral aneurysm initiation. *Stroke* 2007; 38: 1924–1931.

158. Steinman DA. Image-based computational fluid dynamics modeling in realistic arterial geometries. *Ann Biomed Eng* 2002; 30: 483–497.

159. Stuhne GR and Steinman DA. Finite-element modeling of the hemodynamics of stented aneurysms. *J Biomech Eng* 2004; 126: 382–387.

160. Appanaboyina S, Mut F, Löhner R, et al. Computational fluid dynamics of stented intracranial aneurysms using adaptive embedded unstructured grids. *Int J Num Meth Fluids* 2008; 57: 475–493.

161. Castro MA, Putman CM and Cebral JR. Patient-specific computational fluid dynamics modeling of anterior communicating artery aneurysms: a study of the sensitivity of intra-aneurysmal flow patterns to flow conditions in the carotid arteries. *Am J Neuroradiol* 2006; 27: 2061–2068.

162. Cebral JR, Mut F, Raschi M, et al. Aneurysm rupture following treatment with flow-diverting stents: computational hemodynamics analysis of treatment. *Am J Neuroradiol* 2011; 32: 27.

163. Jou LD, Lee DH, Morsi H, et al. Wall shear stress on ruptured and unruptured intracranial aneurysms at the internal carotid artery. *Am J Neuroradiol* 2008; 29: 1761–1767.

164. Xiang J, Natarajan SK, Tremmel M, et al. Hemodynamic–morphologic discriminants for intracranial aneurysm rupture. *Stroke* 2010; 42: 144.

165. Boussel L, Rayz V, McCulloch C, et al. Aneurysm growth occurs at region of low wall shear stress. *Stroke* 2008; 39: 2997.

166. Raschi M, Mut F, Byrne G, et al. CFD and PIV analysis of hemodynamics in a growing intracranial aneurysm. *Int J Num Meth Biomed Eng* 2012; 28: 214–228.

167. Brooks DE, Goodwin JW and Seaman GV. Interactions among erythrocytes under shear. *J Appl Physiol* 1970; 28: 172.

168. Shojima M, Oshima M, Takagi K, et al. Magnitude and role of wall shear stress on cerebral aneurysm. *Stroke* 2004; 35: 2500.

169. Isaksen JG, Bazilevs Y, Kvamsdal T, et al. Determination of wall tension in cerebral artery aneurysms by numerical simulation. *Stroke* 2008; 39: 3172.

170. International Committee for Standardization in Haematology. Recommendation for a selected method for the measurement of plasma viscosity. *J Clin Pathol* 1984; 37: 1147.

171. Khan MO, Chnafa C, Gallo D, et al. On the quantification and visualization of transient periodic instabilities in pulsatile flows. *J Biomech* 2017; 52: 179–182.

172. Valen-Sendstad K, Piccinelli M and Steinman DA. High-resolution computational fluid dynamics detects flow instabilities in the carotid siphon: implications for aneurysm initiation and rupture?. *J Biomech* 2014; 47: 3210–3216.

173. Valen-Sendstad K, Mardal KA and Steinman DA. High-resolution CFD detects high-frequency velocity fluctuations in bifurcation, but not sidewall, aneurysms. *J Biomech* 2013; 46: 402–407.

174. Khan MO, Steinman DA and Valen-Sendstad K. Non-Newtonian versus numerical rheology: Practical impact of shear-thinning on the prediction of stable and unstable flows in intracranial aneurysms. *Int J Num Meth Biomed Eng* 2017; 33(7): e2836.

175. Alibenyahia B, Lemaitre C, Nouar C, et al. Revisiting the stability of circular Couette flow of shear-thinning

fluids. *J Non-Newtonian Fluid Mech* 2012; 183–184: 37–51.

176. Nouar C, Bottaro A and Brancher JP. Delaying transition to turbulence in channel flow: revisiting the stability of shear-thinning fluids. *J Fluid Mech* 2007; 592: 177–194.

177. Peixinho J, Nouar C, Desaubry C, et al. Laminar transitional and turbulent flow of yield stress fluid in a pipe. *J Non-Newtonian Fluid Mech* 2005; 128: 172–184.

178. Moin P and Mahesh K. Direct numerical simulation: a tool in turbulence research. *Annual Rev Fluid Mech* 1998; 30: 539–578.

179. Moser RD, Kim J, Mansour NN, et al. Direct numerical simulation of turbulent channel flow up to Reτ = 590 low Reynolds number modeling with the aid of direct simulation data. *Phys Fluids* 1999; 11: 943–945.

180. Rogallo RS and Moin P. Numerical simulation of turbulent flows. *Ann Rev Fluid Mech* 1984; 16: 99–137.

181. Eggels JGM, Unger F, Weiss MH, et al. Fully developed turbulent pipe flow: a comparison between direct numerical simulation and experiment. *J Fluid Mech* 2006; 268: 175–210.

182. Le H, Moin P and Kim J. Direct numerical simulation of turbulent flow over a backward-facing step. *J Fluid Mech* 1997; 330: 349–374.

183. Kasagi N. Progress in direct numerical simulation of turbulent transport and its control. *Int J Heat Fluid Flow* 1998; 19: 125–134.

184. Coleman G. Similarity statistics from a direct numerical simulation of the neutrally stratified planetary boundary layer. *J Atmos Sci* 1999; 56: 891–900.

185. Scardovelli R and Zaleski S. Direct numerical simulation of free-surface and interfacial flow. *Ann Rev Fluid Mech* 1999; 31: 567–603.

186. Jain K. *Transition to turbulence in physiological flows: direct numerical simulation of hemodynamics in intracranial aneurysms and cerebrospinal fluid hydrodynamics in the spinal canal*. Universi – Universitätsverlag Siegen, 2016.

187. Wilcox DC. *Turbulence modeling for CFD*. DCW Industries, Incorporated, 1994, La Cañada Flintridge, CA, USA.

188. Georgescu A. *Hydrodynamic stability theory*. Netherlands: Springer, 2013.

189. Avila K, Moxey D, De Lozar A, et al. The onset of turbulence in pipe flow. *Science* 2011; 333: 192–196.

190. Eckhardt B. Transition to turbulence in shear flows. *Physica A: Stat Mech Appl* 2018; 504: 121–129.

191. Hwang J and Sung HJ. Wall-attached structures of velocity fluctuations in a turbulent boundary layer. *J Fluid Mech* 2018; 856: 958–983.

192. Priymak VG. Direct numerical simulation of quasi-equilibrium turbulent puffs in pipe flow. *Physics Fluids* 2018; 30(6): 064102.

193. Özahi E and Çarpinlioğlu MÖ. Devised application of LabView for an automatic test system based on generation, control and processing of pulsatile pipe flows. *Isi Bilimi Ve Teknigi Dergisi/ J Thermal Sci Technol* 2015; 35: 75–88.

194. Stettler JC and Hussain AKMF. On transition of the pulsatile pipe flow. *J Fluid Mech* 2006; 170: 169–197.

195. Trip R, Kuik DJ, Westerweel J, et al. An experimental study of transitional pulsatile pipe flow. *Phys Fluids* 2012; 24: 014103.

196. Xu D and Avila M. The effect of pulsation frequency on transition in pulsatile pipe flow. *J Fluid Mech* 2018; 857: 937–951.

197. Brindise MC and Vlachos PP. Pulsatile pipe flow transition: flow waveform effects. *Phys Fluids* 2018; 30: 015111(13).

198. Ford MD and Piomelli U. Exploring high frequency temporal fluctuations in the terminal aneurysm of the basilar bifurcation. *J Biomech Eng* 2012; 134: 091003(10).

199. Gambaruto AM and João AJ. Flow structures in cerebral aneurysms. *Comput Fluids* 2012; 65: 56–65.

200. Sunderland K, Haferman C, Chintalapani G, et al. Vortex analysis of intra-aneurismal flow in cerebral aneurysms. *Comput Math Meth Med* 2016; 2016: 7406215(16).

201. Jou LD and Mawad ME. Timing and size of flow impingement in a giant intracranial aneurysm at the internal carotid artery. *Med Biol Eng Comput* 2011; 49: 891–899.

202. Riccardello GJ Jr., Changa AR, Al-Mufti F, et al. Hemodynamic impingement and the initiation of intracranial side-wall aneurysms. *Intervention Neuroradiol* 2018; 24: 288–296.

203. Brina O, Ouared R, Bonnefous O, et al. Intra-aneurysmal flow patterns: Illustrative comparison among digital subtraction angiography, optical flow, and computational fluid dynamics. *Am J Neuroradiol* 2014; 35: 2348–2353.

204. Lauric A, Hippelheuser J, Safain MG, et al. Curvature effect on hemodynamic conditions at the inner bend of the carotid siphon and its relation to aneurysm formation. *J Biomech* 2014; 47: 3018–3027.

205. Einav S and Sokolov M. An experimental study of pulsatile pipe flow in the transition range. *J Biomech Eng* 1993; 115: 404–411.

206. Xu D, Warnecke S, Song B, et al. Transition to turbulence in pulsating pipe flow. *J Fluid Mech* 2017; 831: 418–432.

207. Carty G, Chatpun S and Espino DM. Modeling blood flow through intracranial aneurysms: a comparison of Newtonian and non-Newtonian viscosity. *J Med Biol Eng* 2016; 36: 396–409.

208. Xiang J, Tremmel M, Kolega J, et al. Newtonian viscosity model could overestimate wall shear stress in intracranial aneurysm domes and underestimate rupture risk. *J Neurointervention Surg* 2012; 4: 351–357.

209. Frolov SV, Sindeev SV, Liepsch D, et al. Experimental and CFD flow studies in an intracranial aneurysm model with Newtonian and non-Newtonian fluids. *Technol Health Care* 2016; 24: 317–333.

210. Hippelheuser JE, Lauric A, Cohen AD, et al. Realistic non-Newtonian viscosity modelling highlights hemodynamic differences between intracranial aneurysms

with and without surface blebs. *J Biomech* 2014; 47: 3695–3703.

211. Sano T, Ishida F, Tsuji M, et al. Hemodynamic differences between ruptured and unruptured cerebral aneurysms simultaneously existing in the same location: 2 Case reports and proposal of a novel parameter oscillatory velocity index. *World Neurosurg* 2017; 98: 868.e865–868.e810.

212. Otani T, Ii S, Hirata M, et al. Computational study of the non-Newtonian effect of blood on flow stagnation in a coiled cerebral aneurysm. *Nihon Reoroji Gakkaishi* 2017; 45: 243–249.

213. Xiang J, Tremmel M, Kolega J, et al. Newtonian viscosity model could overestimate wall shear stress in intracranial aneurysm domes and underestimate rupture risk. *J Neurointervention Surg* 2012; 4: 351–357.

214. Morales HG, Larrabide I, Geers AJ, et al. Newtonian and non-Newtonian blood flow in coiled cerebral aneurysms. *J Biomech* 2013; 46: 2158–2164.

215. Owen I, Gray J, Escudier M and Poole R. The importance of the non-Newtonian characteristics of blood in flow modelling studies. In: *The Second Physiological Flow Network Meeting*, University of Edinburgh, Scotland 2005 Sep, pp. 26–27.

216. Gosselin D, Huet M, Cubizolles M, et al. Viscoelastic capillary flow: the case of whole blood. *AIMS Biophys* 2016; 3: 340–357.

217. Pipe CJ, Majmudar TS and McKinley GH. High shear rate viscometry. *Rheologica Acta* 2008; 47: 621–642.

218. Kuchar NR and Ostracn S. Unsteady entrance flows in elastic tubes with application to the vascular system. *AIAA J* 1971; 9: 1520–1526.

219. Ling SC, Atabek HB, Letzing WG, et al. Nonlinear analysis of aortic flow in living dogs. *Circulat Res* 1973; 33: 198–212.

220. Back LD, Radbill JR and Crawford DW. Analysis of pulsatile, viscous blood flow through diseased coronary arteries of man. *J Biomech* 1977; 10: 339–353.

221. Lutz RJ, Cannon JN, Bischoff KB, et al. Wall shear stress distribution in a model canine artery during steady flow. *Circulat Res* 1977; 41: 391–399.

222. Tóth BK, Raffai G and Bojtár I. Analysis of the mechanical parameters of human brain aneurysm. *Acta Bioeng Biomech* 2006; 7: 3–22.

223. Hayashi S, Funahashi K, Itakura T, et al. Significance of hemodynamic stress on the development of intracranial aneurysms – analysis of the cases of coexisting intracranial aneurysm and arteriovenous malformation of the brain. *Neurologia Medico-Chirurgica* 1982; 22: 219–226.

224. Lansman JB, Hallam TJ and Rink TJ. Single stretch-activated ion channels in vascular endothelial cells as mechanotransducers? *Nature* 1987; 325: 811–813.

225. Olesen S-P, Claphamt D and Davies P. Haemodynamic shear stress activates a K + current in vascular endothelial cells. *Nature* 1988; 331: 168–170.

226. Davies PF. Flow-mediated endothelial mechanotransduction. *Physiol Rev* 1995; 75: 519–560.

227. DePaola N, Gimbrone MA Jr, Davies PF, et al. Vascular endothelium responds to fluid shear stress gradients. *Arteriosclerosis Thromb* 1992; 12: 1254–1257.

228. Tzima E, Irani-Tehrani M, Kiosses WB, et al. A mechanosensory complex that mediates the endothelial cell response to fluid shear stress. *Nature* 2005; 437: 426–431.

229. Valencia AA, Guzmán AM, Finol EA, et al. Blood flow dynamics in saccular aneurysm models of the basilar artery. *J Biomech Eng* 2006; 128: 516–526.

230. Berg P, Abdelsamie A, Janiga G, et al. Multi-phase blood flow modelling in an intracranial aneurysm considering possible transition to turbulence. In: *International symposium on turbulence and shear flow phenomena, TSFP 2013*, Sunriver, Oregon, USA, June 26–29, 2013.

231. Varble N, Trylesinski G, Xiang J, et al. Identification of vortex structures in a cohort of 204 intracranial aneurysms. *J Royal Soc Interface* 2017; 14. Article. DOI: 10.1098/rsif.2017.0021.

232. Jayaraman T, Paget A, Shin YS, et al. TNF-α-mediated inflammation in cerebral aneurysms: a potential link to growth and rupture. *Vasc Health Risk Manage* 2008; 4: 805–817.

233. Steinman DA, Milner JS, Norley CJ, et al. Image-based computational simulation of flow dynamics in a giant intracranial aneurysm. *Am J Neuroradiol* 2003; 24: 559–566.

234. Meckel S, Stalder AF, Santini F, et al. In vivo visualization and analysis of 3-D hemodynamics in cerebral aneurysms with flow-sensitized 4-D MR imaging at 3 T. *Neuroradiology* 2008; 50: 473–484.

235. Isoda H, Ohkura Y, Kosugi T, et al. In vivo hemodynamic analysis of intracranial aneurysms obtained by magnetic resonance fluid dynamics (MRFD) based on time-resolved three-dimensional phase-contrast MRI. *Neuroradiology* 2010; 52: 921–928.

236. Schnell S, Ansari SA, Vakil P, et al. Three-dimensional hemodynamics in intracranial aneurysms: Influence of size and morphology. *J Magnetic Resonance Imag* 2014; 39: 120–131.

237. Blankena R, Kleinloog R, Verweij BH, et al. Thinner regions of intracranial aneurysm wall correlate with regions of higher wall shear stress: a 7T MRI study. *Am J Neuroradiol* 2016; 37: 1310–1317.

238. Zhang X, Yao ZQ, Karuna T, et al. The role of wall shear stress in the parent artery as an independent variable in the formation status of anterior communicating artery aneurysms. *European radiology* 2019; 29(2): 689–698 (in press). DOI: 10.1007/s00330-018-5624-7.

239. Boussel L, Rayz V, Martin A, et al. Phase-contrast magnetic resonance imaging measurements in intracranial aneurysms in vivo of flow patterns, velocity fields, and wall shear stress: comparison with computational fluid dynamics. *Magnetic Resonance Med* 2009; 61: 409–417.